CHALMERS | UNIVERSITY OF GOTHENBURG

PREPRINT 2012:23

Laplace moving average model for multi-axial responses in fatigue analysis of a cultivator

MATS KVARNSTRÖM
KRZYSZTOF PODGÓRSKI
IGOR RYCHLIK

Department of Mathematical Sciences
Division of Mathematical Statistics
CHALMERS UNIVERSITY OF TECHNOLOGY
UNIVERSITY OF GOTHENBURG
Gothenburg Sweden 2012

Preprint 2012:23

Laplace moving average model for multi-axial responses in fatigue analysis of a cultivator

Mats Kvarnström, Krzysztof Podgórski
and Igor Rychlik

Department of Mathematical Sciences
Division of Mathematical Statistics
Chalmers University of Technology and University of Gothenburg
SE-412 96 Gothenburg, Sweden
Gothenburg, November 2012

Preprint 2012:23
ISSN 1652-9715

Matematiska vetenskaper
Göteborg 2012

Laplace moving average model for multi-axial responses in fatigue analysis of a cultivator

MATS KVARNSTRÖM*, KRZYSZTOF PODGÓRSKI** AND IGOR RYCHLIK***
Adresses:
* FCC, SE- Gothenbourg, Sweden
mats.kvarnstrom@fcc.chalmers.se
** Statistics, Lund University, 220 07 Lund, Sweden
krzysztof.podgorski@stat.lu.se
*** Mathematical Sciences, Chalmers University of Technology, SE-412 96 Göteborg, Sweden (Corresponding author)
rychlik@chalmers.se

Abstract

Modeling of loads on a vehicle through Laplace moving averages is extended to the multivariate setting and efficient methods of computing the damage indexes are discussed. Multivariate Laplace moving averages are used as statistical models of multi-axial loads represented by forces and moments measured at some locations of a cultivator. As oppose to models based on the Gaussian distribution, these models account explicitly for transients that have a common origin – vibrations that can be caused by large obstacles encountered by a cultivator or a vehicle driving into potholes. The model is characterized by a low number of parameters accounting for fundamental characteristics of multivariate signals: the covariance matrix representing size of loads and their mutual dependence, the excess kurtosis that in the model is related to relative size of transients, and the time scale that accounts for the vehicle speed. These parameters can be used to capture diversity of environmental conditions in which the vehicle operates. Distributions of parameter values that are specific to a given market or encountered by specific customers can be then used to describe the long term loading. The model is validated by analysis of the resulting multi-axial damage index. It is shown that the parameters enter this index in a multiplicative and explicit manner and, for a given damage exponent, only the factor representing dependence on the kurtosis has to be obtained through regression approximation based on Monte Carlo simulations. An example of actual cultivator data are used to illustrate the accuracy of damage and fatigue life prediction.

Keywords: damage variability, multi-axial rainflow, Laplace moving averages, multi-axial loads.

1 Introduction

This study is focused on modeling vibrations of a cultivator and stresses occurred as a result of encountered load. Durability characteristics of vehicle components often require a customer or market specific load description. Variability of stresses depends on many factors such as a type of equipment, speed, maneuvering topography of a field, a type of soil, etc. For example, when a cultivator is working in heavy soil its vibrations can be quite accurately described by means of locally stationary Gaussian processes. In contrast, when it is operating in light sandy soils where stones are frequent, the vibrations have larger spread of variation that can not be any longer modeled by solely Gaussian processes. This is mostly due to the fact that transients caused by encountered obstacles are frequent and may become the main reason for the ensuing fatigue and damage.

The importance for accurate modeling of such working environment is highlighted by the evidence of greater fatigue damage in cultivator's components comparing to the ones caused by stresses following Gaussian models. To obtain an accurate while not over-parameterized model of the environment and resulting loads we consider the class of general Laplace moving averages (LMA) – the processes that have been discussed, for example, in [1]. In [2], the fatigue damage rates for loads modeled as Gaussian moving averages were compared with the damage rates computed under a Laplace noise. Such LMA loads have kurtosis exceeding the value of three – the necessary value for Gaussian loads – and a considerable increase of the fatigue damage accumulation rate was reported for higher values of

kurtosis. This effect from the model is in agreement with empirical evidence.

Here we propose a multivariate extension of the hybrid model introduced in [5] that characterizes soil by two parameters; the intensity of transients (obstacles) μ and the parameter ν measuring their sizes. The value $\nu = 0$ leads to the Gaussian model while large ν causes the fatigue process to be dominated by transients with large amplitudes. Both Gaussian vibrations and transients depend also on cultivator properties. These enter the model through square integrable kernels $g(t)$ defining the moving average processes and hence the power density functions of the response components.

The material is organized as follows. First the damage index related to the so called multi-axial rainflow count introduced in [4] is reviewed in Section 2. In Section 3, we define load as a moving average over a random noise, both the Gaussian case and a more general case of LMA are discussed. Some properties of LMA essential for fatigue damage modeling are discussed and exemplified. A representation of the model that explicitly involves transients is discussed in Section 4, where also a scaling property of the expected damage is presented. The univariate hybrid model that combines Gaussian and Laplace moving averages is introduced in Section 5. Section 6 is devoted to multivariate extensions of the models and a property is presented that shows that under suitable assumptions the expected damage resulting from a multi-hybrid model thataxial load can be expressed by the univariate expected damage. In Section 7, the multivariate hybrid models are fit to multi-axial loads measured in a cultivator. Finally, formal arguments supporting the results of the paper are detailed in the appendix together with MATLAB code to simulate multivariate hybrid models.

2 Multiaxial fatigue damage

In this work, a multivariate random process $\mathbf{X}(t) = (X_1(t), \ldots, X_M(t))$ represents multi-axial loads containing transients, where X_i's represent forces and bending moments acting on a structure at different locations. For a stiff structure, stresses used to predict fatigue damages are linear combinations of forces and moments. For this reason, it is important to model the multi-axial load so that a stress, i.e. a linear combination of loads

$$Y_{\mathbf{a}}(t) = \sum_{r=1}^{M} a_r X_r(t), \qquad t \in [0, T], \tag{1}$$

yields accurate fatigue accumulation. Since the vector $\mathbf{a} = (a_1, \ldots, a_M)$ may vary between locations in a structure experiencing the same loads $\mathbf{X}(t)$ one requires good accuracy for any choice of the vector $\mathbf{a}$. The fatigue damage accumulated in material is expressed using a fatigue (damage) index defined by means of the rainflow method which is computed in the following two steps. First rainflow ranges h_k^{rfc}, $k = 1, \ldots, K$ in $Y_{\mathbf{a}}(t)$ are found, then the rainflow damage is computed according to Palmgren-Miner rule [11], [10], viz.

$$D_\beta(\mathbf{a}) = \frac{1}{T} \sum_{k=1}^{K} (h_k^{rfc}(\mathbf{a}))^\beta, \tag{2}$$

see also [13] for details of this approach. Various choices of the damage exponent β can be considered but in this paper most often $\beta = 3$ which is the standard value for the crack growth process. For comparison we also consider $\beta = 5$ that is often used when fatigue process is dominated by crack initiation phase. The index $D_\beta(\mathbf{a})$ is often called multi-axial damage intensity and was first introduced in [4], see also [14] and [12].

The proposed model for multi-axial load $\mathbf{X}(t)$ is validated by using measured loads and comparing the ensuing damage index with the expected value of the damage index following from the model fitted to the data. In this, first the model parameters are fit using measured loads $\mathbf{X}^{obs}(t)$, then the expected theoretical damage index

$$\mathcal{D}_\beta(\mathbf{a}) = \mathsf{E}\left[D_\beta(\mathbf{a})\right] \tag{3}$$

is estimated by means of Monte Carlo (MC) method and compared with $D_\beta^{obs}(\mathbf{a})$ for a suitably chosen vector of factors $\mathbf{a}$ and β, where $D_\beta^{obs}(\mathbf{a})$ is computed by means of (2) with rainflow ranges obtained

in the observed records. In our notation we do not explicitly indicate that the expected damage index $\mathcal{D}_\beta(\mathbf{a})$ depends also on the properties and defining parameters of the process $\mathbf{X}$. In what follows, whenever this dependence needs to be exhibited, we write $D_\beta^{\mathbf{X}}(\mathbf{a})$ and $\mathcal{D}_\beta^{\mathbf{X}}(\mathbf{a})$ for the damage and the expected damage, respectively .

3 Laplace moving averages model for loads

In this section we review some facts about the LMA models. In what follows, the response is denoted by $X(t)$ and is normalized to have mean zero and variance one. We start by reviewing the standard Gaussian moving averages.

A zero mean stationary Gaussian process is completely defined by its spectral density and thus any probability statement about properties of Gaussian loads can be in principle expressed by means of the spectral density. This is not always practically possible and hence MC methods are often employed to estimate probabilities of interest. There are several ways to generate Gaussian sample paths. The algorithm proposed in [17] is often used in engineering and it is based on the spectral representation of a stationary process. Here we use an alternative way to generate Gaussian processes employing moving averages of a Gaussian white noise. The method naturally extends to Laplace moving averages (LMA) by simply replacing the Gaussian noise by a Laplace distributed white noise, see e.g. [2], [5], for more details.

In an approximate sense, a general moving average process is the convolution of a kernel function $g(t)$ with a infinitesimal "white noise" process having variance equal to the discretization step, say dt. The kernel $g(t)$ is normalized so that its square integrates to one, which is equivalent to saying that the variance of $X(t)$ is one. In particular, the standardized (mean zero and variance one) Gaussian moving average (GMA) can be written as

$$X(t) = \int_{-\infty}^{+\infty} g(t-u)\, dB(u) \approx \sum_{i=-\infty}^{\infty} g(t-t_i) Z_i \sqrt{dt}, \tag{4}$$

where $B(t)$ is a Brownian motion independently extended to the past, Z_i's are independent standard Gaussian variables, t_i are discretization points chosen regularly and densely enough over $(-\infty, \infty)$ with the discretization step dt. The approximation is valid due to $\Delta B(t_i) = B(t_i + dt) - B(t_i) = \sqrt{dt} Z_i$. A choice of appropriate length of the increment dt is related to smoothness of the kernel. In the example of Section 7, the reciprocal of the sampling frequency of 500 Hz is used, i.e. $dt = 0.002$ [s].

There is an important relation between the kernel and the spectrum of a moving average process

$$S_X(\omega) = \frac{1}{2\pi} |\mathcal{F}g(\omega)|^2, \tag{5}$$

where $\mathcal{F}g(\omega)$ stands for the Fourier transform. While in general this relation does not allow for unique identification of the kernel for a given spectrum, if we limit ourselves to the kernels symmetric around zero, i.e. such that $g(-t) = g(t)$, they can be defined through their Fourier transform by

$$\mathcal{F}g(\omega) = \sqrt{2\pi\, S_X(\omega)}. \tag{6}$$

It is worth to note here that there are many asymmetric kernels that give the same spectrum since equation (5) does not have a unique solution in g. Moreover, while for the Gaussian processes any of the kernels (symmetric or not) satisfying (5) defines the same GMA, this is not the case for LMA and the choice of a kernel may have important consequences for the model, see also Example 3.

In the simplest terms, a LMA is obtained by replacing the deterministic standard deviation of the Gaussian noise $\sqrt{dt}$ by random $\sqrt{K_i}$, where independent gamma distributed variables K_i are chosen so that the variance of $\sqrt{K_i} Z_i$ is the same as that of $\sqrt{dt} Z_i$, i.e. so that $\mathsf{E}[K_i] = dt$. This is achieved by taking in the gamma distribution the shape parameter dt/ν and scale $\nu > 0$. The new model for

$X(t)$ can be approximately written as

$$X(t) \approx \sum_{i=-\infty}^{\infty} g(t-t_i) Z_i \sqrt{K_i}. \tag{7}$$

The variables $\Lambda_i = \sqrt{K_i}\, Z_i$ have the generalized symmetric Laplace distribution, sometimes also called the Bessel function distribution, with scale $\sqrt{\nu}$ and the shape parameter dt/ν. Due to an explicit form of the characteristic function, see [8], the moments of a generalized Laplace distribution are readily available and the parameter ν can be estimated using the method of moments from excess kurtosis κ_e of X:

$$\nu = \frac{\kappa_e}{3 \int g(t)^4\, dt}. \tag{8}$$

If the discretization step dt tends to zero the process in (7) is formally an approximation of

$$X(t) = \int_{-\infty}^{+\infty} g(t-u)\, d\,\Lambda(u), \tag{9}$$

where $d\Lambda(u)$ is the symmetric Laplace noise process with the shape parameter ν and $\mathbb{V}ar\,(d\Lambda(t)) = dt$, see [1] for further details. Note that when the shape parameter ν decreases to zero LMA becomes GMA. MATLAB code to generate LMA/GMA can be found in [5]. In the following section we shall motivate how the parameter ν relates to the relative magnitudes of transients in loads.

4 LMA process as a model for load transients

One can interpret the approximation (7) as a transient process that adds transients $g(t-t_i)Z_i\sqrt{K_i}$ at the discretization points t_i. More precisely, one can limit t_i only to $[0,T]$ for appropriately large T and consider values of t that are not 'too close' to the end points of this interval so that the following approximation is accurate

$$X(t) \approx \sum_{i=1}^{N} Z_i \sqrt{K_i} g(t-t_i), \tag{10}$$

where N is the integer part of T/dt and $t_i = idt$. Thus a LMA process essentially represents the effects of jumps (shocks) as the resulting loads is the sum of transients caused by the jumps. The transients have the shape of the kernel that is scaled by the jump sizes.

The above can be formalized since from the mathematical point of view a sequence of jumps occurring in time constitutes the Laplace motion as seen in the following series expansion

$$\Lambda(t) = \sum_{i=1}^{\infty} Z_i \sqrt{K_i^*}\, \mathbf{1}_{[0,U_i]}(t),\ 0 \le t \le T, \tag{11}$$

where Z_i's are independent standard Gaussian variables, U_i are independent uniformly on $[0,T]$ distributed locations of jumps, and $\mathbf{1}_{[0,U]}$ stands for the indicator function of an interval $[0,U]$. The random factors K_i^* are given by

$$K_i^* = \nu\, W_i\, e^{-\nu\gamma_i/T}. \tag{12}$$

where W_i are i.i.d. standard exponential variables independent of Z_i and U_i. Finally, γ_i is the location of the i-th point in a Poisson process, i.e., $\gamma_i = \sum_{j=1}^{i} G_j$, where G_j are independent standard exponential distributed random variables independent of all previously introduced variables, cf. [6].

Using the series expansion (11) of $\Lambda(t)$, the LMA load $X(t)$ in (9) is approximated by the following series expansion

$$X(t) \approx \sum_{i=1}^{\infty} Z_i \sqrt{K_i^*} \cdot g(t-U_i). \tag{13}$$

This representation resembles (10) but it differs in two aspects. Firstly, the t_i's that are regularly spaced over $[0,T]$ have been replaced by the U_i's which are independently and uniformly distributed over the

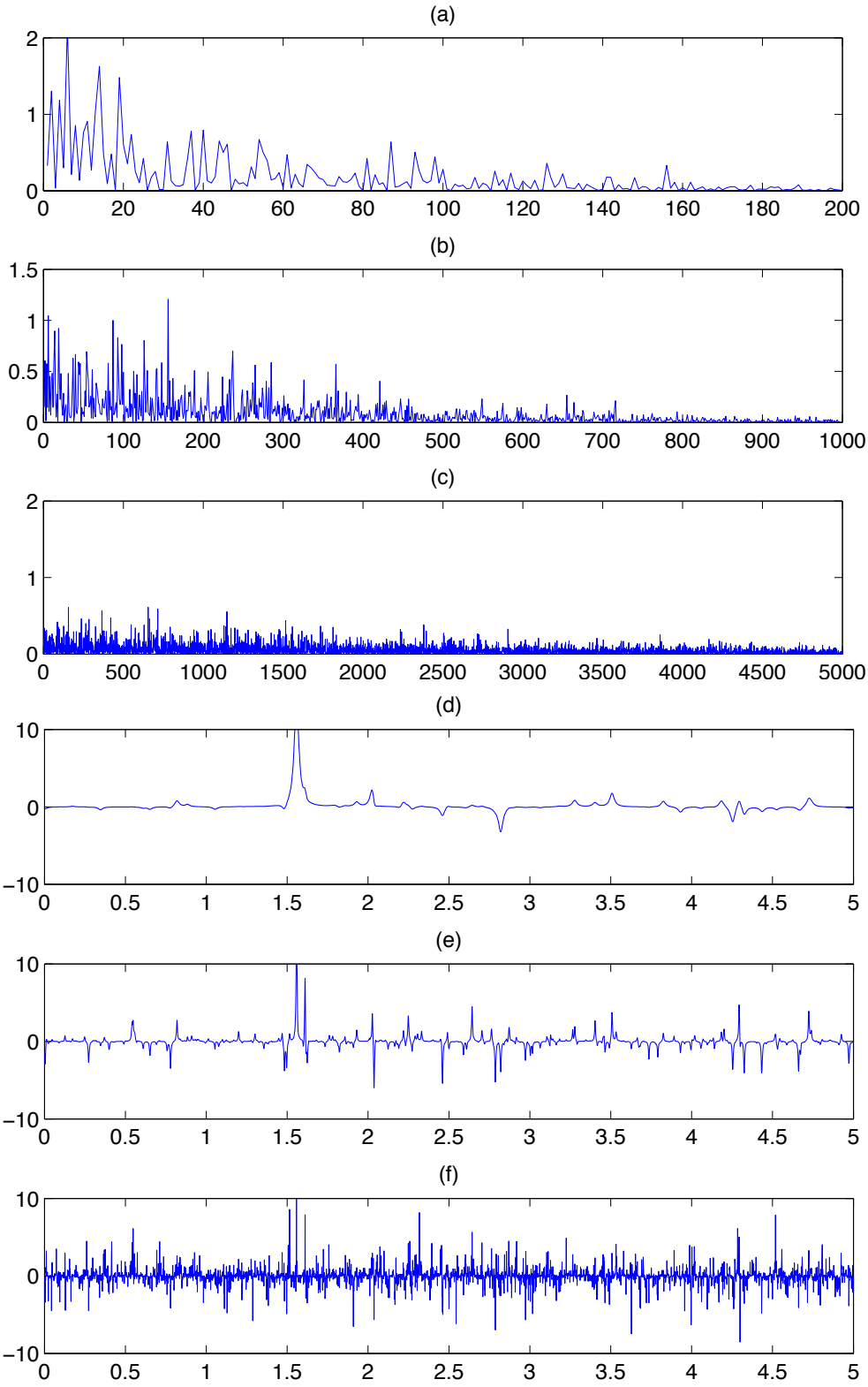

Figure 1: *Top a)-c):* The factors K_i^*, $i = 1, \ldots, k$, where $k = 200, 1000, 5000$ for parameter $\nu = 0.5, 0.1, 0.01$, respectively. *Bottom d)-f):* LMA processes having kurtosis 10 and exponential spectrum (15) with s equal to 0.17, 0.034 and 0.0034, and the K_i^* sequences given in the top three graphs, respectively. In generating K_i^* values for each of the three cases, the same values of random variables γ_i's and W_i's are used and only ν is varying.

same interval. Secondly, the independent sizes of transients $\sqrt{K_i}Z_i$ at regularly spaced and ordered points t_i have been replaced by 'partially ordered' $\sqrt{K_i^*}Z_i$ at random points U_i. This 'partial ordering' is due to $e^{-\nu\gamma_i/T}$ in (12) being a strictly decreasing sequence in i, see also Figure 1 a)-c).

The expansion of Laplace process is approximately valid for large T and for these values of t for which

$$X(t) = \int_{-\infty}^{+\infty} g(t-u)\, d\,\Lambda(u) \approx \int_0^T g(t-u)\, d\,\Lambda(u).$$

The range of T and t for accurate approximation can be identified through the second order accuracy condition

$$1 - \int_0^T g^2(t-u)\, du \approx 0.$$

This is because the left hand side of the above is equal to $\mathbb{V}ar\left(X(t) - \int_0^T g(t-u)\, d\,\Lambda(u)\right)$.

Representation (13) shows that for $\nu > 0$ the response is a sum of transients uniformly (and independently) located in time while the sizes of the transients have a distribution parametrized by ν. The average amplitude of a transient is given by

$$\mathsf{E}\left[|Z_i|\sqrt{K_i^*}\right] = \frac{\sqrt{2\nu}}{(1+\nu/2T)^i} \approx \sqrt{2\nu}\, e^{-\nu\, i/2T}, \tag{14}$$

which demonstrates that the mean value of the transient in the series representation is exponentially decaying. A LMA process with large ν is locally dominated by a few transients with very large amplitudes, while low values of ν mean that the sizes of transients are less variable and LMA is closer to a Gaussian model.

The dependence of transient sizes K_i^* on parameter ν is illustrated in Figure 1 a)-c), where a number of larger K_i^*'s are shown for $\nu = 0.5, 0.1, 0.01$, for the top to bottom plots, respectively. The values K_i^* presented in the graphs are computed using (12) with the same values of random variables γ_i and W_i. Only ν is varying in (12) so that the three sequences are functionally dependent in order to illustrate better the role of ν. We see clearly that ν plays a role of a time scale parameter (rate), which is explained in further detail in Appendix B.

Example 1 (Exponential spectrum – the leading example of LMA).

As a useful illustration, we discuss a LMA with an exponential spectrum. The spectrum is parameterized by a scale parameter $s > 0$, viz.

$$S_s(w) = 0.5\, s \exp(-s|w|) \tag{15}$$

and for shortness $S(w) = S_1(w)$, so that $S_s(w) = sS(sw)$. In Section 7, we shall use this spectrum to model cultivator loads in sandy soil with stones.

By using (5) and some well-known formulas for the Fourier transform, we obtain the corresponding symmetric kernel function

$$g_s(t) = \frac{2}{\sqrt{s\pi}} \frac{1}{1+(2t/s)^2}. \tag{16}$$

We denote $g(t) = g_1(t)$ so that $g_s(t) = g(t/s)/\sqrt{s}$. Note that for any natural n:

$$\int_{-\infty}^{+\infty} g_s(t)^n\, dt = s^{1-n/2}\, \frac{\Gamma(n-1/2)}{\Gamma(n)} \left(\frac{2}{\sqrt{\pi}}\right)^{n-1}. \tag{17}$$

Consequently the parameter ν, given by (8), is proportional to excess kurtosis κ_e and s, viz.

$$\nu = 0.4189\, \kappa_e\, s. \tag{18}$$

In Figure 1 d)-f), three LMA loads $X_r(t)$, $r = 1, 2, 3$ with exponential spectra all having kurtosis 10 are presented for three cases of the Laplace noise: $\nu = 0.5, 0.1, 0.01$. The three noises are presented in Figure 1 a)-c). Consequently, by (18), the exponential kernels have parameter $s = 0.17,\ 0.034,$

0.0034, respectively. The difference between the responses is striking but is mostly due to differences in spikiness of the used kernels – smaller values of s lead to more "spiky" kernels.

The values of K_i^*'s for each of the three loads are computed using (12) with the same values of random variables γ_i and W_i and only the parameter ν is altered by assuming values 0.5, 0.1 and 0.001, respectively. Further the Gaussian variables Z_i, used in (13) were taken the same for all three cases. Thus there is in fact a functional dependence between obtained samples. The dependence between $X_r(t)$ and $X_k(t)$ is nonlinear but its linear component is summarized through the correlation coefficient

$$\rho_{rk} = \frac{\int_0^T g_r(t-x)g_k(t-x)\,dx}{\sqrt{\int_0^T g_r^2(t-x)\,dx \int_0^T g_k^2(t-x)\,dx}} \approx \int_0^T g_r(t-x)g_k(t-x)\,dx,$$

where $g_r(t) = g(t/s_r)/\sqrt{s_r}$, $r = 1, 2, 3$ and $s_1 = 0.17$, $s_2 = 0.034$, $s_3 = 0.0034$. The choice of t in the above integrals should be such that they do not significantly differ from the ones with the limits of integration extended to the entire real line (which would make the integral independent of t). For this choice of the parameters, the correlations are: $\rho_{12} \approx 0.75$, $\rho_{13} \approx 0.28$, $\rho_{23} \approx 0.58$.

This section is concluded with a discussion of a method for evaluating the expected damage for the LMA process, see also [15]. We start with a general result that demonstrates a convenient scaling property of the expected damage for the LMA processes. We consider the LMA model $X_\nu(t)$ which has its statistical properties uniquely given by two characteristics:

a) a kernel $g(t)$ that is normalized so that its squared integral equals to one (and thus the variance of $X_\nu(t)$ is also equal to one),

b) the parameter ν controlling relative sizes of the transients occurring in the Laplace motion as represented in (11).

We note that for the process $X_\nu(t)$ the expected damage satisfies

$$\mathcal{D}_\beta^{X_\nu}(a) = a^\beta \mathcal{D}_\beta^{X_\nu}(1).$$

Definition 1. *The expected damage for the standard model relatively to the density g (the dependence on which is not shown in the notation) is defined as*

$$d_\beta(\nu) \stackrel{def}{=} D_\beta^{X_\nu}(1). \tag{19}$$

The model is then extended by addition of the scale parameter s in the kernel, so that we deal with a family of kernels $g_s(t) = g(t/s)/\sqrt{s}$. This extended model is denoted by $X_{\nu,s}(t)$. Note that g_s still integrates to one and in the corresponding spectrum s also plays the role of a scale because $S_s(\omega) = sS(s\omega)$, where S_s, S are spectra of $X_{\nu,s}(t)$, $X_\nu(t)$, respectively.

The following result is a consequence of scaling properties of the Laplace motion and the formal argument are provided in Appendix B.

Proposition 1. *With the introduced notation, the expected damage as function of s, a, and ν has the form*

$$\mathcal{D}_\beta^{X_{s,\nu}}(a) = \frac{a^\beta}{s} d_\beta(\nu/s). \tag{20}$$

From the result it follows that for a fixed β in order to compute the expected damage one needs only establish the dependence of the expected damage for the standard model on the parameter ν, i.e. to determine the function $\nu \mapsto d_\beta(\nu)$. For this purpose we employ non-linear regression applied to the damages obtained from Monte Carlo simulations of loads from the model. This is illustrated in Figure 2 *Top-Left* for the case of exponential spectra (15) parameterized by the scale s while the damage exponent is $\beta = 5$. In this figure one can see that the simulated damage indexes are spread around the fitted line. The residuals may seem large which is caused by short lengths of simulations but we found it more accurate to use several simulations for the same value of parameter ν instead of single but very long one. Eventually in this particular case the expected damage was approximated by

$$d_5(\nu) = 91.04 + 888.8\nu - 1895\nu^{1/2} + 1284\nu^{1/3}. \tag{21}$$

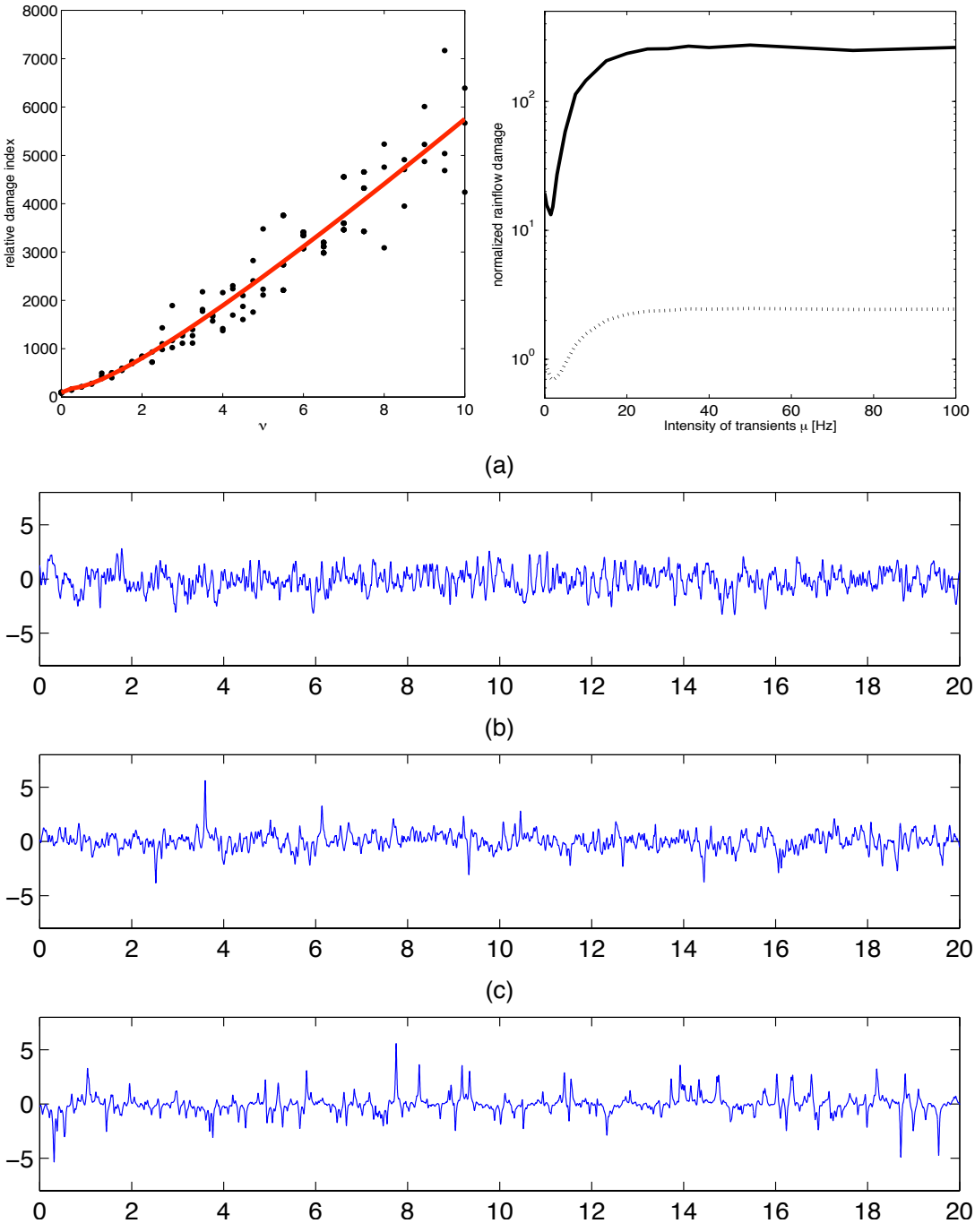

Figure 2: *Top-Left:* Regression fit (solid line) to the simulated damage indexes $d_\beta(\nu)$ for a LMA process defined by the kernel (16) with $s = 1$. The dots represent values of $d_\beta(\nu)$ using simulated samples of $X(t)$. *Top-Right:* Dependence of the damage on the intensity of transients. The damages are scaled so that the expected damage index for the Gaussian load with $\mu = 0$ and $\beta = 3$ is one. The dashed line represents the expected damage indexes for $\beta = 3$ while the solid line corresponds to the indexes for $\beta = 5$. *Three bottom graphs:* (a) intensity of transients $\mu = 0$, i.e. Gaussian model; (b) $\mu = 5$, i.e. Gaussian load with 100 transients added; (c) $\mu = 20$, i.e. Gaussian load with 400 transients added.

5 The hybrid model

In practice, Gaussian processes are often used to model "normal" loads to which one is adding transients caused by impulse forces acting on a structure. Since such an approach is physically appealing, we propose to alter the LMA model so that it will resemble this general scheme. The process is called the hybrid model and formally is defined in the next paragraph, while the main idea is as follows. In the transient/jump series representation of the previous section given in (13), we deal with infinite number of terms which in any practical application has to be replaced by a finite partial sum. In the hybrid model, we contain in such a sum the most dominant and influential transients, see Figure 1 a)-c), while the sum of all remaining small ones is replaced by a Gaussian process.

First we introduce one more parameter $\mu > 0$ which we will call the intensity of transients. Then the normalized (mean zero, variance one) load $X(t)$, $0 \leq t \leq T$, is defined by

$$X(t) = pZ_0(t) + \sum_{i=1}^{k} Z_i(t), \quad p \in [0,1], \tag{22}$$

where $k = \mu T$ is the number of 'influential' transients, $Z_0(t)$ is the zero mean variance one Gaussian process having spectrum S_X defined in (5), while $Z_i(x)$'s are taken from the transient representation of LMA as

$$Z_i(t) = Z_i \sqrt{K_i^*}\, g(t - U_i). \tag{23}$$

The constant p is chosen in such a way that $\mathsf{V}[X(t)] \approx 1$ and employing approximation (41) of Appendix A, we obtain a relation between p and μ:

$$p^2 = e^{-\nu k/T} = e^{-\nu\,\mu}. \tag{24}$$

Thus to specify the hybrid model with a given kernel it is enough to find (estimate) μ in (24) and from the above relation the parameter p can be determined. The Gaussian process $p\,Z_0(t)$, p defined in (24) is seen as a 'normal' load to which one adds transients occurring with intensity μ. On one hand, introducing an additional parameter, which has to be estimated, increases the uncertainty in the estimated damage. On the other hand the parameter μ can be conveniently used to tune up the model. In many situations the Gaussian model ($\mu = 0$) leads to underestimation of damage while the LMA model ($\mu = \infty$) is conservative. Hence one can use μ to reduce the bias.

Example 2. This example shall illustrate how damage depends on intensity of transients. A response X with exponential spectrum, introduced in Example 1, having parameter $s = 0.034$, is used. Further X has kurtosis $\kappa = 10$ and hence by (18) $\nu = 0.1$. First we visually compare hybrid models with increasing intensity of transients.

The three bottom graphs of Figure 2 show the components of the simulated hybrid model X with increasing intensity of transient μ. In plot (a) $\mu = 0$, i.e.the hybrid model X is just a Gaussian process. It should be compared with plots (b) and (c), where 100 respectively 400 transients are added. One can see that in the plot (c) transients are dominating in the sense that variability of the process is smaller between the transients comparing what can be seen in plots (a) and (b).

Secondly in Figure 2 *(Top-Right)*, the dependence of the damage index on intensity of transient μ is illustrated. The expected damage indexes are estimated for two damage exponents $\beta = 3, 5$. The indexes are scaled so that it is one for the Gaussian load ($\mu = 0$) and damage exponent $\beta = 3$. In the figure one can see that the damage grows relatively fast with the intensity of transients μ to the asymptotically level, which for the damage exponent $\beta = 3$ is about 2.1 while for $\beta = 5$ the the level is about 14.3.

6 Multi-axial loading

In many fatigue applications loads are uni-axial and can be modeled by means of a one dimensional random process. However, there are situations when the uni-axiality of a load can not be assumed. In these cases, it is crucial, for accuracy of fatigue life prediction, that the joint variability of loads is

well described by a multivariate process. If the multi-axial loads are jointly Gaussian, then any linear combination of the loads is Gaussian too and there are several methods to evaluate the corresponding damage index. In a non-Gaussian case, extending from uni-axial loads to multi-axial ones becomes a much more difficult problem. A common approach is to consider the loads as transformed multivariate Gaussian processes, see e.g. [18], [19], [16] and [3]. However, if the loads contain transients, then the transformed Gaussian models are not applicable because the Gaussian processes fundamentally can not account for jumps. Instead, to model transients in multi-axial loads, we propose to use a correlated LMA process that was introduced in [9].

We start with the most general form of a multivariate LMA process. This new multi-axial model is an extension of (13) to the multivalued case, viz.

$$X_r(t) \approx \sum_{i=1}^{\infty} \tilde{Z}_{ir} \sqrt{K^*_{ir}} \cdot g_r(t - U_i),\ r = 1, \ldots, M \tag{25}$$

where, with the notation of (12),

$$K^*_{ir} = \nu_r\, e^{-\nu_r \gamma_i / T}\, W_i, \tag{26}$$

and $\tilde{\mathbf{Z}}_i = (\tilde{Z}_{i1}, \ldots, \tilde{Z}_{iM})$ is a sequence of Gaussian vectors such that $\tilde{\mathbf{Z}}_i$ and $\tilde{\mathbf{Z}}_j$ are independent for $i \neq j$ but the vector coordinates are correlated. More precisely, let $\mathbf{Z}_i = (Z_{i1}, \ldots, Z_{iM})$ be a sequence of standard Gaussian vectors with independent coordinates and $\mathbf{\Sigma}$ be $M \times M$ covariance matrix. Then

$$\tilde{\mathbf{Z}}_i = \sqrt{\mathbf{\Sigma}} \mathbf{Z}_i, \tag{27}$$

where $\sqrt{\mathbf{\Sigma}}$ is any matrix such that $\mathbf{\Sigma} = \sqrt{\mathbf{\Sigma}} \sqrt{\mathbf{\Sigma}}^T$. For further properties of this model we refer to [9].

Let us note several important properties of the proposed model.

- Each coordinate process $X_r(t)$ constitutes a univariate LMA process with time scale ν_r responsible for the relative size of transients, and kernel $g_r(t)$.
- The random variances $(K^*_{ir})_{i \in \mathbb{N}}$ of the transient sizes of the loads $X_r(t)$'s for various r are dependent since their randomness is determined solely by γ_i's and W_i's and these are taken the same for all loads.
- In the case of $\mathbf{\Sigma}$ equal to the identity matrix and conditionally on the variances K^*_{ir}, the loads are independent since the variables Z_{ir} are mutually independent. As one consequence, the loads are uncorrelated but they are not independent because the presence of the same variables γ_i's and W_i's will be visible in the transients sizes across all loads. Therefore the matrix $\mathbf{\Sigma}$ introduces the correlation between the sizes of transients in the coordinates of the multi-axial records.
- The time scale parameters ν_j can be different for different loads and constitute one of the two main sources of the difficulty in evaluating the expected damage index for linear combination of the loads, see the discussion in Appendix C. Different forms of the kernels g_r are the second source of the difficulty.

Enumeration of the expected damage $\mathcal{D}^{\mathbf{X}}_{\beta}(\mathbf{a})$ although computationally challenging, is still within range of computing power of a desktop computer, see Appendix C. More importantly, the numerical difficulties can be reduced significantly under certain simplifying assumptions that are discussed next.

If the loads are measured in the same environment, the relative sizes of the transients observed in the loads should be similar. It has been also noted that their variability little affects the ensuing damage. Therefore it is reasonable to simplify the model by assuming that all ν_r's are equal to some common value, say, ν. On the other hand if different ν_r's represent different operating environments that this can be accounted by a hierarchical model with some fitted distribution of, now random, ν_r. When evaluating the expected damaged over environments represented by the distribution of ν_r, one can consider the Gaussian first order approximation and replace various ν_r by the common expected value $\nu = E(\nu_r)$.

Frequently, we can also find a common kernel $g(t) = g_r(t)$ for all axial loads. This is another realistic while simplifying assumption that can be also interpreted through averaging a hierarchical model. Under these two assumptions we have the following property that significantly simplifies evaluation of the expected damage.

Proposition 2. *For the multi-axial LMA load $\mathbf{X} = \mathbf{X}_\nu$ given by (25) having covariance function $\mathbf{\Sigma}$ and a common time scale parameter (relative size of transients) ν with a common kernel g, the following relation holds*

$$\mathcal{D}_\beta^{\mathbf{X}}(\mathbf{a}) = \left(\mathbf{a}^T \mathbf{\Sigma} \mathbf{a}\right)^{\beta/2} d_\beta(\nu).$$

For the argument see Appendix C.

We see that the computation of the expected damage is reduced to the uni-axial case which has to be done numerically and was discussed at the end of Section 4. In the model, the correlation matrix $\mathbf{\Sigma}$ between the damage indexes of the components in a multi-axial load has to be estimated. Given the kernels this can be done using the straightforward relation between the covariance of the process, the kernel, and the matrix $\mathbf{\Sigma} = [\sigma_{rk}]_{r,k=1,\ldots,M}$:

$$\mathbb{C}ov\left(\mathbf{X}(t), \mathbf{X}(0)\right) = \left[g_r * \tilde{g}_k(t) \cdot \sigma_{rk}\right]_{r,k=1,\ldots,M}, \tag{28}$$

where $*$ stands for the convolution operator and $\tilde{g}(s) = g(-s)$, see [9] for details. If it is assumed that the kernels for the uni-axial components are the same, i.e. $g_r(t) = g(t)$, $r = 1, \ldots, M$, then we obtain a convenient relation that can be used for estimation of $\mathbf{\Sigma}$:

$$\mathbb{C}ov(\mathbf{X}(t), \mathbf{X}(0)) = g * \tilde{g}(t)\, \mathbf{\Sigma}.$$

As in the one dimensional case, see Section 5, the multivariate hybrid model is obtained by truncating infinite sums in (25) at $k_r = \mu_r\, T$, where μ_r are the intensities of the transients, and approximating the truncation errors by means of Gaussian processes, viz.

$$Z_r(t) = p_r Z_{0r}(t) + \sum_{i=1}^{k_r} Z_{ir}(t), \quad p_r \in [0, 1]. \tag{29}$$

Here $Z_{0r}(t)$ are correlated zero mean variance one Gaussian process having spectrum S_{X_r}, while $Z_{ir}(x)$'s are defined as before using formula (25), viz.

$$Z_{ir}(t) = Z_{ir} \sqrt{K_{ir}^*} \cdot g_r(t - U_i) \tag{30}$$

Constants p_r are chosen in such a way that $\mathbb{V}ar Z_r(t) \approx 1$, and hence, employing approximation (41),

$$p_r^2 = e^{-\nu_r k_r / T} = e^{-\nu_r \mu_r}. \tag{31}$$

Example 3.

In the example we consider two correlated processes $X_1(t), X_2(t)$ having different both kurtoses and kernels. The general model for process $X_1(t)$ was considered in Section 1, Example 1. It has the exponential spectrum with parameter $s = 0.05$ and kurtosis $\kappa = 20$, i.e. the scale parameter of Laplace noise is $\nu = 0.7$ and the symmetric kernel $g_1(t)$ given in (16) is assumed.

The process $X_2(t)$ is the response of a linear damped oscillator driven by a white noise process. The response has a power spectrum

$$S_X(\omega) = m^{-2} \frac{1}{(\omega_0^2 - \omega^2)^2 + 4\alpha^2\omega^2} \tag{32}$$

and is a solution to the following standardized differential equation

$$\ddot{X}(t) + 2\zeta\omega_0 \dot{X}(t) + \omega_0^2 X(t) = m^{-1}\Lambda(t), \tag{33}$$

where $\Lambda(t)$ is the Laplace white noise given in (11). Here $\alpha = \zeta\omega_0$, $\tilde{\omega}_0 = \omega_0\sqrt{1 - \zeta^2}$. The symmetric kernel can be obtained from (6), however here we will use a causal kernel given by the filters impulse response function

$$g_2(t) = m^{-1}\tilde{\omega}_0^{-1} e^{-\alpha\, t} \sin(\tilde{\omega}_0\, t), \quad t \geq 0, \tag{34}$$

and zero otherwise. The Fourier transform of g_2 is

$$\left(\mathcal{F} g_2\right)(\omega) = m^{-1} \frac{1}{-\omega^2 + 2\zeta i \omega_0\, \omega + \omega_0^2}$$

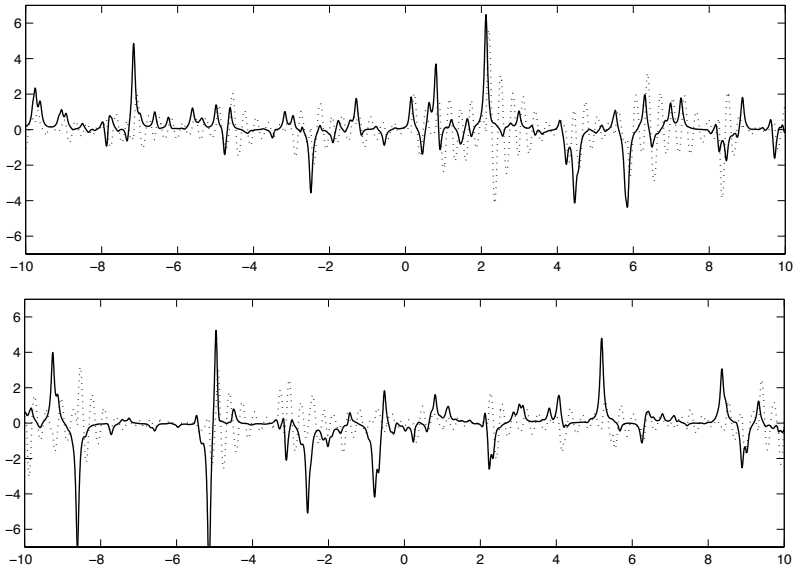

Figure 3: Segments of loads $X_1(t)$ and $X_2(t)$. The solid line corresponds to $X_1(t)$ having exponential spectrum while the dashed line shows $X_2(t)$ that is an output of linear oscillator driven by a Laplace noise. *Top:* Transient are correlated $\rho = 0.9$. *Bottom:* Uncorrelated sizes of transients, $\rho = 0$.

and hence by (5) it yields the spectrum in (32). In the example, the parameters are $\zeta = 0.1$, $\omega_0 = 20$, $m = 1/80$ and kurtosis $\kappa = 10$ which gives parameter $\nu = 0.9$. The correlation between the transients (represented in the general model by $\mathbf{\Sigma}$) is set to $\rho = 0.9$.

We simulated 100 pairs of processes $X_1(t), X_2(t)$. In Figure 3 (upper plot) a fragment of one such simulation is presented. The process X_1 is drawn using a solid line while X_2 is shown by a dashed line. One can see that large transients in both functions start at the same location and that their amplitudes are correlated. However, the correlation between signals is quite low, viz. $\mathbb{C}orr(X_1(t), X_2(t)) = 0.27$ that is computed from (28). It is much smaller value than the correlation between the sizes of transients: $\rho = 0.9$.

Next we illustrate that the correlation between damage indexes should be confused neither with $\mathbf{\Sigma}$ nor with $\mathbb{C}orr(X_1(t), X_2(t))$. For the multi-axial fatigue, it is more important to accurately model the dependence between the damages than the one between the processes. Using 100 simulations, the damages indexes have been computed in X_1 and X_2 for damage exponents $\beta = 3$ and $\beta = 5$. The correlations between the damages were 0.8 and 0.74 for $\beta = 3, 5$, respectively, which are quite high and not far from the correlation between the transients amplitudes $\rho = 0.9$. Finally, for the choice of parameters and damage exponents, the expected damage indexes for X_2 were 1.2, when $\beta = 3$, and 2.7, for $\beta = 5$, times higher than the expected damage indexes for $X_1(t)$.

Finally in Figure 3 (lower plot), $X_1(t), X_2(t)$ simulated with uncorrelated transients sizes $\rho = 0$ are shown. It follows clearly from (28) that $X_1(t), X_2(t)$ are uncorrelated. However, one can observe in the records that they are statistically dependent illustrating the fact that the Laplace models, in contrast to the Gaussian ones, can be uncorrelated but still dependent.

7 Modeling cultivator loads

7.1 Data

The multivariate LMA model has been used to describe variability of forces and moments measured on a cultivator working in harsh conditions, i.e. sandy soil with stones. Loads are six dimensional, three forces and three moments. However, we observed directly in the data that only the forces $F_y(t)$, $F_z(t)$ and of the moments $M_x(t)$, $M_y(t)$ are not negligible. The data set consists of 18 measured multi-axial loads for tines working at the depth of 10 cm in the soil. The duration of signals are about 15 seconds

and sampled with frequency 500 Hz. The damage indexes, defined in (2), computed for M_x, M_y are much smaller than the damage indexes for F_y and F_z hence, arbitrarily, the bending moments has been neglected in the analysis. Consequently in this particular case, we shall model a bi-axial load $(F_y(t), F_z(t))$, fit and then validate it by means of the 18 measurements.

Univariate modeling of $F_z(t)$ for a similar data set consisting of 12 time segments was discussed in [15]. It was demonstrated that the LMA with an exponential spectrum can be used to model the force and that the damage index was highest for LMA with the symmetric kernel. Based on these results, we shall use a "conservative" approach and model the measured signals by symmetric kernels, given in (16). We keep the parameter s and the kurtosis the same for both the components of the considered bivariate load so that the average damage index for multivariate load can be computed by means of Propositions 1 and 2. In the following examples an empirical formula for $d_\beta(\nu)$, $\beta = 3$, derived in [15] through the regression approach discussed also in Section 4, is used

$$d_3(\nu) = 4.84 + 0.06\nu + 8.32\nu^{1/2} - 5.15\nu^{1/3}, \tag{35}$$

where $d_3(\nu)$, given in (19), is defined for X_ν having symmetric kernel (16) and exponential spectrum (15), with $s = 1$. We note that in our examples, we do not use the hybrid model since $\mu = 500$ which for all practical reason removes the Gaussian part of the hybrid model, therefore here $d_3(\nu)$ does not depend on μ.

7.2 Hierarchical model for parameter values

There are 18 bivariate data $(F_y(t), F_z(t))$, which in the generic notation of the previous sections correspond to realizations of $\mathbf{X}(t) = (X_1(t), X_2(t))$. To remain in the domain of applicability of Proposition 2, it is required that the relative size of transients represented by ν and the scale s of the exponential kernel are the same for uni-axial signal X_1 and X_2. In a more general approach, one could allow both s and ν to differ between X_1 and X_2 but, as discussed below, the data suggest that this is not necessary and thus, as an important consequence, allowing for simplified computation of the damage following from the results of this paper. All in all, our model for the bi-axial records is parameterized by the total of 5 parameters: the time scale s and relative size of transients ν, variances σ_1^2 and σ_2^2, and correlation ρ.

It is observed that when each of 18 biaxial records is considered individually, statistical estimates of these parameters are relatively accurate as measured by standard deviation of the estimation error and considering their short lengths (only 15 seconds). Thus the statistical fit of the model to the data appears to be reasonable. However, the accuracy of the model in a single run of experiment does not guarantee statistically consistent fits between runs. In the terminology of the design of experiments, the run of experiment can be a (nuisance) factor representing some unaccounted influences of experimental settings. This effect is also described in mathematical theory as non-ergodicity of the model. In a stationary but non-ergodic model the long time averages (estimates) are convergent to non-constant, random values, and this randomness represents certain model unaccounted factors occurring during each run of the experiment.

One way to build this into the model is by introducing a hierarchical structure in which the parameters of the LMA model are sampled from a certain distribution at each run of the experiment. In order to determine if there is a justified need for the hierarchical model, stability of the model for different runs of the experiment has to be investigated. To address this important question we have analyzed 18 different runs of the experiment to check the between-run variability of kurtosis and variances.

Let us start our discussion of the performed numerical study with comments on estimation of the spectrum scale s. The estimation methods discussed in [15] have been applied to the eighteen runs of bivariate measurements yielding 36 estimates of s obtained from the univariate records. The means of the estimates of s yielded 0.0101, 0.0084, respectively for each force. Since the standard deviation for the difference between the scale parameters is 0.0024, we conclude that the scale parameters do not differ significantly and hence it can be assumed that both forces will have the same common estimated value 0.0092 of s. The between run variation has been verified by utilizing Monte Carlo analysis of variability of estimates. Using simulation algorithm described in Appendix D, twenty Monte Carlo samples have been generated from the model with parameters taken from each of the 18 fits of the

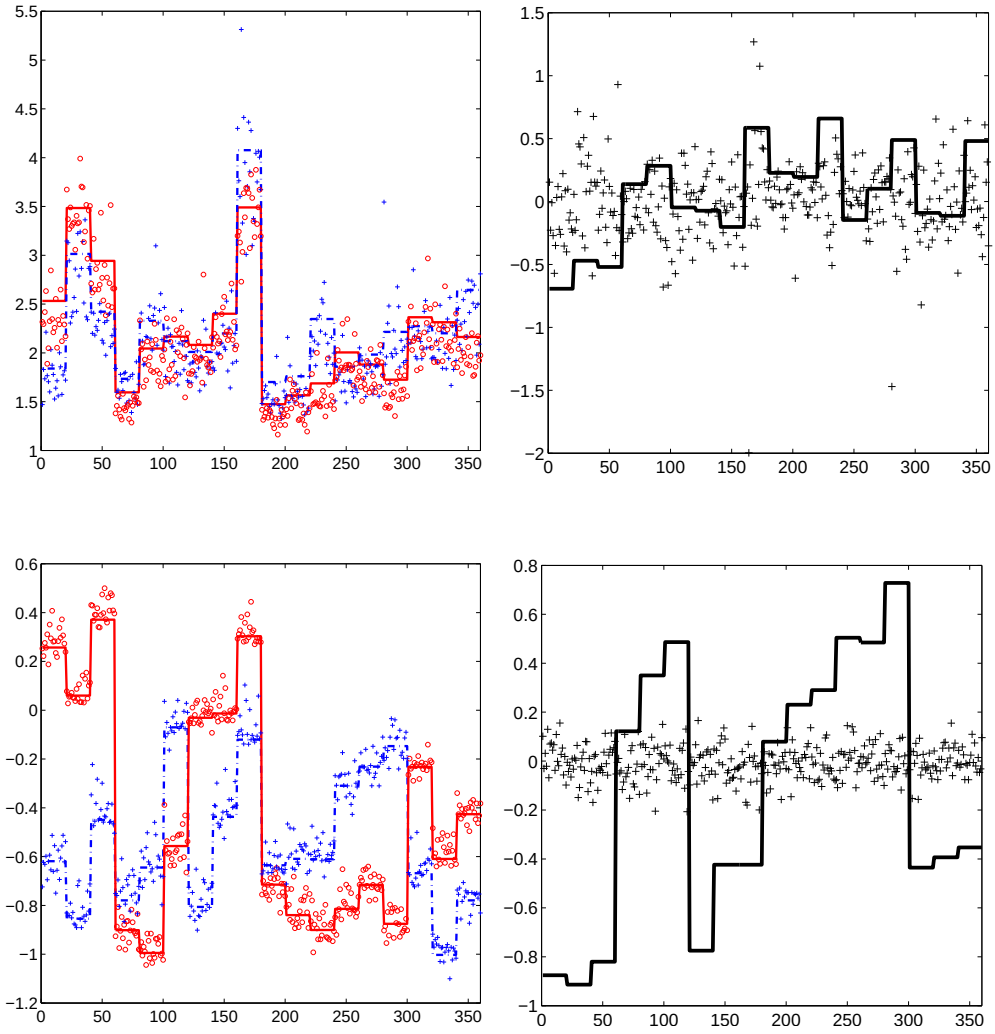

Figure 4: A study between run variability of the model. *Top-Left:* Logarithms of estimates of kurtosis in 18 in loads F_y (dashed-dotted line), F_z (solid line) plotted together with Monte Carlo log-values of the estimates (crosses – F_y ; circles – F_z). *Top-Right:* The differences of the estimates from the left hand side plot. *Bottom:* Analogous plots for the variance estimates.

model based on the actual data. For each of these Monte Carlo samples, the parameters of the model have been fit again and their variability was investigated and compared with the variability between estimates for 18 runs of the experiment.

In Figure 4, we illustrate some of the performed analyzes. The estimates of kurtosis *(Top)* and variances *(Bottom)* for each of 18 signals are represented in the plots by piecewise constant graphs. In the left hand side top plot, there are two such lines representing the 18 estimates of kurtosis (expressed in their logarithms), one (dot-dashed) for F_y and the other (solid) corresponding to F_z. One can observe that the kurtosis variability in-between runs is evidently larger than the one within the run observed in the Monte Carlo simulations of estimates (crosses for F_y and circles for F_z). We conclude that the hierarchic model with respect to the kurtosis is needed to fully account for this variation. In the right hand side figure we confront the differences between kurtosis estimates for the empirical signals (piecewise constant continuous line graph) and the corresponding differences obtained from the Monte Carlo samples. The variability of those differences does not appear to be significantly different from the Monte Carlo variability verifying that the assumption of equal kurtosis (and thus of ν) is not contradicted by the empirical data.

Similarly, in the bottom plots, we illustrate estimation of variances σ_1 and σ_2. Here it is evident

that differences between estimates of the two force variances each of the forces are significantly non-zero and a proper model for the data would require a different variance for each force. We also observe significant between-run differences which calls for a hierarchical model with respect to variance. On the other hand, we found that taking individually estimated correlation for each signal does not essentially affects the accuracy of model fitting, so we opted for a common value of the correlation for all runs.

In the conclusion of this subsection, it is worth to mention that while the structure of hierarchical models resembles the Bayesian models in this that the parameters are assumed to come from a certain distribution (in the Bayesian terminology called the prior distribution), the two approaches should not be confused. An important methodological distinction is that while the distributions of the parameters in the Bayesian approach are somewhat arbitrarily chosen with fundamental inability for its empirical verification, in the hierarchical models we actually have different runs of experiments that can be used for statistical verification of the assumptions on the parameter distributions.

7.3 LMA modelling of (F_y, F_z), 10 cm tines depth

As we have seen in the previous subsection, there is a strong indication that variable parameters for each run of the experiment are needed both for the common kurtosis of the two forces represented (indirectly) by ν and their individual variances σ_z^2 and σ_y^2. In the hierarchical model, we consider a probabilistic distribution $p(\nu, \sigma_z, \sigma_y)$ on these parameters and compute the total expected damage as

$$\mathcal{D}_{total} = \int \mathcal{D}_\beta^{\mathbf{X}}(\mathbf{a}; \nu, \sigma_z, \sigma_y) p(\nu, \sigma_z, \sigma_y) d\nu d\sigma_z d\sigma_y, \tag{36}$$

where the explicit dependence of the damage on the parameters represented in the hierarchical model is shown in the notation. When working with empirical data, one could replace $p(\nu, \sigma_z, \sigma_y)$ by its empirical equivalent obtained from sample distribution of the fitted parameters $(\hat{\nu}_i, \hat{\sigma}_{z,i}, \hat{\sigma}_{y,i})$, $i = 1, \ldots, K$, where in our example $K = 18$.

Despite the documented need for a hierarchical model, it is not clear that the damage itself is sensitive to accounting for such a more complex model. For example, it is worth to verify if the following Gaussian approximation is appropriate

$$\mathcal{D}_{total} \approx \mathcal{D}_\beta^{\mathbf{X}}(\mathbf{a}; \mu_\nu, \mu_{\sigma_z}, \mu_{\sigma_y}), \tag{37}$$

where $\mu_\nu, \mu_{\sigma_z}, \mu_{\sigma_y}$ are the mean values of (functions of) random parameters $(\nu, \sigma_z, \sigma_y)$ with respect to $p(\nu, \sigma_z, \sigma_y)$. In other words, one could investigate if it is reasonable to replace a hierarchical model by a non-hierarchical and thus simpler one with the parameters being averaged values of parameters across different runs of the experiment.

For this purpose, we consider two models for $\mathbf{\Sigma}$. One in which a constant $\mathbf{\Sigma}$ equals to the average estimated from the 18 signals and the other one in which we average correlation between X_1 and X_2 across the records but estimate variance for each signal separately. Additionally, we have considered both varying and constant kurtosis. Here is a summary of models that are considered:

a) all parameters (kernel scale, kurtosis, variance, and covariance) fixed;

b) excess kurtosis and correlation between loads fixed but variable variances;

c) correlation between loads fixed, variable excess kurtosis between 18 records (although the same for X_1 and X_2) and variable variances.

The choice between the alternatives is basically the question of sensitivity of the damage index on variability of the parameters. Two values of the damage exponents are used, $\beta = 3, 5$, and the damage index is computed by means of Propositions 1 and 2. Note that the parameter ν is computed for g_s kernel by means of (18), and hence the damage indexes (utilizing the notation in (20) and taking $\mathbf{a} = (\cos(\theta), \sin(\theta))$) are given by

$$\mathcal{D}_\beta^{\mathbf{X}}(\mathbf{a}) = \mathcal{D}_\beta^{X_\nu}(1) \cdot (\mathbf{a}\,\mathbf{\Sigma}\,\mathbf{a}^T)^{\beta/2} = \frac{(\mathbf{a}\,\mathbf{\Sigma}\,\mathbf{a}^T)^{\beta/2}}{s} d_\beta(\nu/s),$$

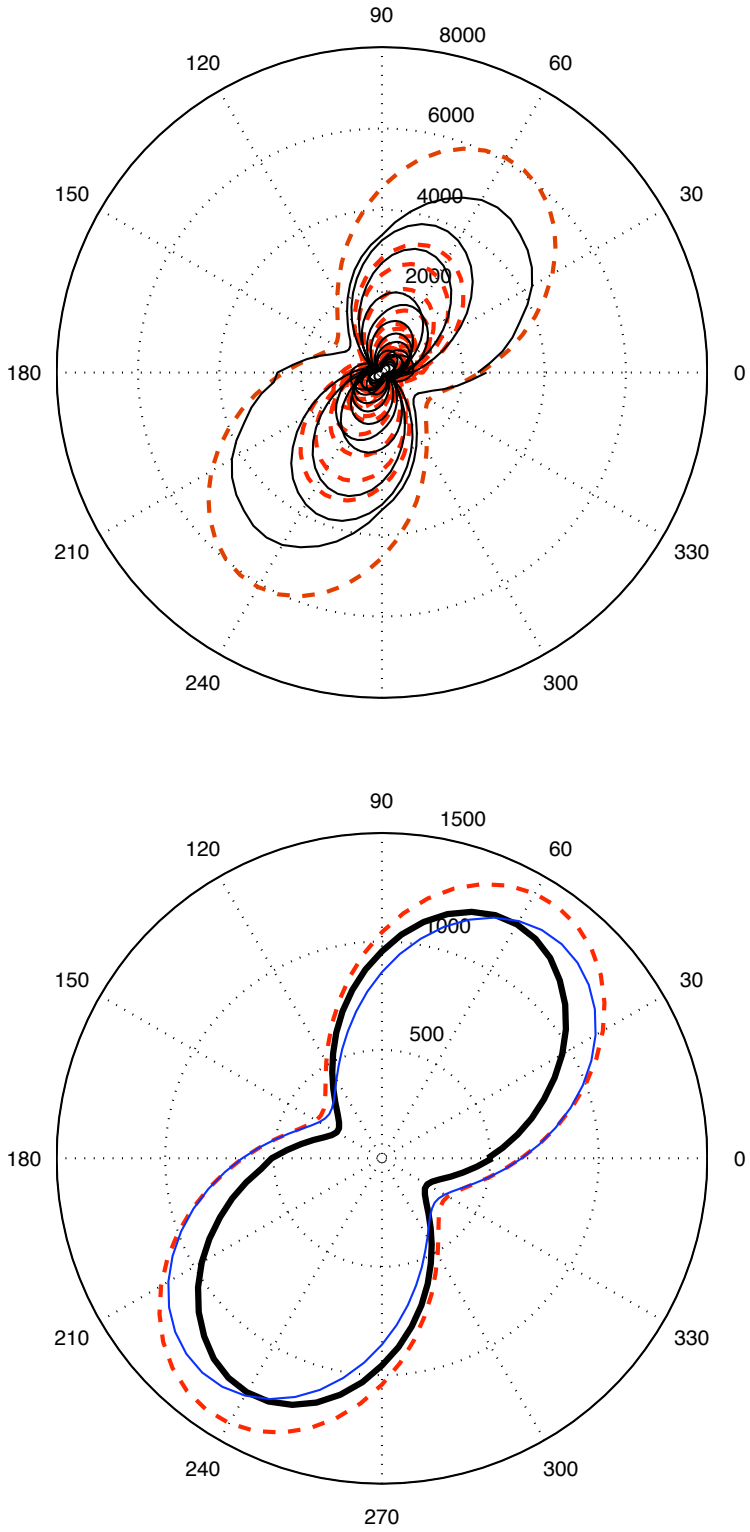

Figure 5: The case of the damage exponent $\beta = 3$. *Top:* Damage of individual records. *Solid lines:* 18 observed damage indexes as function of θ (in the polar coordinates); *Dashed line:* 18 damage indexes computed using Propositions 1 and 2 with observed variances, observed ν, fixed relative scale $s = 0.009$ and fixed correlation $\rho = 0.428$ which is equal to the average correlation estimated from the observed signal (using variable correlation affects results only marginally). *Bottom:* The total damage indexes (over 18 cases): *Solid thick line:* averaged observed; *Dashed line:* average of dashed lines in the top graph; *Solid thin line:* damaged computed using Propositions 1 and 2 with all parameters fixed and equal to the observed averages.

where $d_\beta(\cdot)$ stands, as in (19), for for the expected damage of the standardized LMA corresponding to X_1 (or X_2), i.e. such that the kernel has the scale s equal to one and with the variance equal to one, while ν represents the relative transient sizes. Substituting $\nu/s = 0.419\kappa_e$, we obtain the following formulas

$$\begin{aligned} \mathcal{D}_3(\mathbf{a}) &= s^{-1} \cdot (\mathbf{a}\,\boldsymbol{\Sigma}\,\mathbf{a}^T)^{3/2}(4.84 + 0.025\kappa_e + 3.486\kappa_e^{1/2} - 2.158\kappa_e^{1/3}), \\ \mathcal{D}_5(\mathbf{a}) &= s^{-1} \cdot (\mathbf{a}\,\boldsymbol{\Sigma}\,\mathbf{a}^T)^{5/2}(91.04 + 372.4\kappa_e - 794\kappa_e^{1/2} + 538\kappa_e^{1/3}). \end{aligned} \tag{38}$$

Since the frame of the cultivator is stiff the damage indexes $\mathcal{D}_\beta(\mathbf{a})$ can be used as an indicator of the severity of the loads. The factors $\mathbf{a}$ vary between hot spots and usually are computed using the final element method. In this example, we investigate whether the proposed bi-axial hybrid model adequately predict the observed damage indexes for different factors $\mathbf{a}$. Next, the factors $\mathbf{a} = (\cos(\theta), \sin(\theta))$, $0 \le \theta \le \pi$, were used. Consequently, the damage indexes in the following 18 signals were computed

$$Y_i^{obs}(t;\theta) = \cos(\theta)F_{y,i}(t) + \sin(\theta)F_{z,i}(t), \qquad \theta \in [0, 2\pi],$$

and $i = 1, \ldots, 18$. In the following, we shall write $D_\beta^{obs}(\theta)$ for $D_\beta^{obs}(\mathbf{a})$. The eighteen observed damage indexes $D_\beta^{obs}(\theta)$ are shown using continuous lines in the polar coordinates in Figure 5-*top*, where damage exponent $\beta = 3$ is used (an analogous graph for the case of $\beta = 5$ see Figure 6-*top*). They can be compared with the dashed line graphs obtained using Propositions 1 and 2 with the observed variances evaluated individually for each of 18 records.

In Figure 5-*bottom*, three differently computed averages of the total damage are shown. In a thick solid line, we see the simple arithmetic mean of the 18 observed damages. The dashed line shows the analogous mean based on the 18 damages obtained by estimating variance for each signal separately ('averaging' the dashed lines in Figure 5-*top*). Finally, the thin solid line shows the damage obtained by substituting for the model parameters in Propositions 1 and 2 their averaged (over 18 records) estimates. As we can see, the difference between the expected total damages: the observed one, the one computed from (37) and the one from the hierarchical approach given in (36) is negligible, leading us to the conclusion that the simplified computation based on the Gaussian approximation is appropriate.

However, the situation is different for the damage exponent $\beta = 5$. In Figure 6, we see analogous plots to the ones given in Figure 5. Additional illustration in the middle presents the same values as in the top graphs but using the logarithms of the damages in order to show better the agreement of the records for small values of the damages. We can see in the bottom plot that the Gaussian approximation (thin solid line) is not giving accurate damage, while the approach based on the hierarchical model performs much better providing a good and conservative approximation of the damage obtained directly from the empirical records.

8 Conclusions

We propose to use the multivariate Laplace moving average model for muliti-axial loads. Two useful properties of the damage for this model are derived. One deals with the scaling/transient intensity change of the load, while the other demonstrates how the damage resulting from the multivariate load can be reduced to the damage for a univariate load. These properties allow for a straightforward computation of the damage which is utilized in a study of multiaxial loads of a cultivator. The variability of between run variation in the data is accounted through a hierarchical model. An example of biaxial load data for a cultivator is studied. A discussion of sensitivity of the fitted model to the between run variability observed in the experiment is carried out. The obtained results show that the model based damage is quite robust on variability of the parameters in the case of $\beta = 3$, while the higher damage exponent $\beta = 5$ requires the approach through hierarchical model in order to provide accurate estimates of the damage. In general, the multivariate LMA model proves to be useful for studying damages resulting from multiaxial loads. It summarizes in a very small number of parameters important features of the loads that are affecting damage. This efficiency in parameters allows in particular to build in a clear and manageable manner a hierarchical structure that seems to be necessary to explain all variability in the investigated cultivator data.

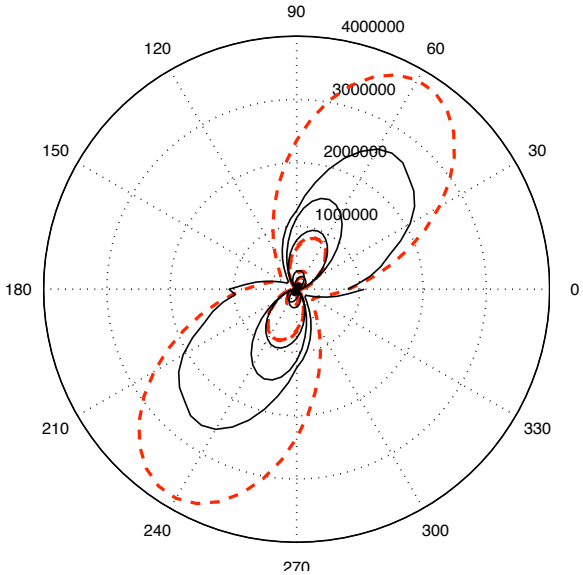

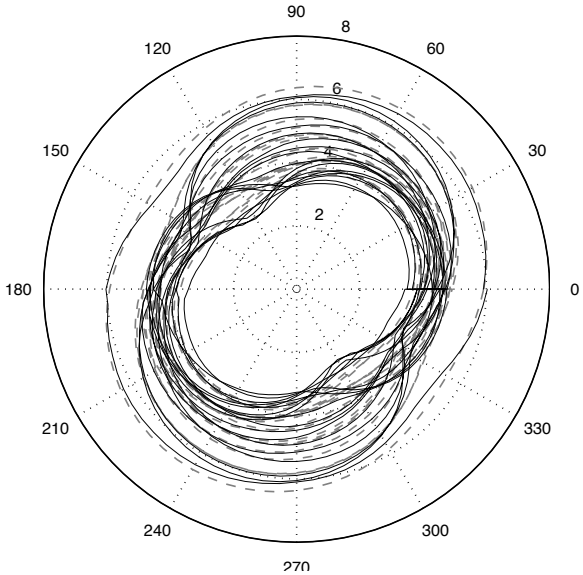

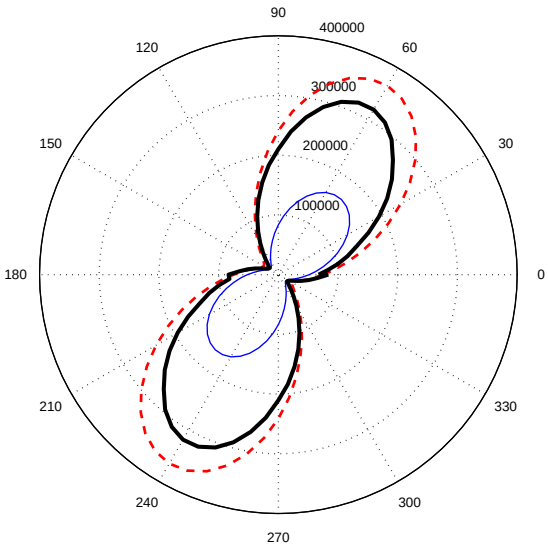

Figure 6: The case of $\beta = 5$. The top and bottom graphs are analogous to the ones in Figure 5, while the middle graph shows the logarithms of damage of individual records in order to present more detail of the individual damages.

9 Acknowledgments

The authors are thankful to Henrik Gunnarsson for discussions and to Väderstad-Verken AB for supplying the cultivator data.

References

[1] S. Åberg and K. Podgórski. A class of non-gaussian second order random fields. *Extremes*, 14:187–222, 2011.

[2] S. Åberg, K. Podgórski, and I. Rychlik. Fatigue damage assessment for a spectral model of non-Gaussian random loads. *Probab. Engin. Mechanics*, 24:608–617, 2009.

[3] J-M. Azais, S. Déjean, J.R. Leon, and F. Zwolska. Transformed gaussian stationary models for ocean waves. *Probab. Engin. Mechanics*, 26:342–349, 2011.

[4] A. Beste, K. Dressler, H. Kötzle, and W.Krüger. Multiaxial Rainflow - A consequent continuation of Professor Tatsuo Endo's work. In Y. Murakami, editor, *The Rainflow Method in Fatigue: The Tatsuo Endo Memorial Volume*. Butterworth-Heinemann, 1992.

[5] K. Bogsjö, K. Podgórski, and I. Rychlik. Models for road surface roughness. *Vehicle System Dynamics*, 50:725–747, 2012.

[6] L. Bondesson. On simulation from infinitely divisible distributions. *Adv. Appl. Prob.*, 14:855–869, 2007.

[7] P.A. Brodtkorb, P. Johannesson, G. Lindgren, I. Rychlik, J. Rydén, and E. Sjö. Wafo - a matlab toolbox for analysis of random waves and loads. In *Proc. 10th Int. Offshore and Polar Eng. Conf., Seattle*, volume 3, pages 343–350, 2000.

[8] S. Kotz, T.J. Kozubowski, and K. Podgórski. *The Laplace Distribution and Generalizations: A Revisit with Applications to Communications, Economics, Engineering and Finance*. Birkhaüser, Boston, New York, 2001.

[9] T.J. Kozubowski, K. Podgórski, and I. Rychlik. Multivariate Laplace moving average fields. *Journal of Multivariate Analysis*, pages 1–25, 2012. In press.

[10] M.A. Miner. Cumulative damage in fatigue. *J. Appl. Mech.*, 12:A159–A164, 1945.

[11] A. Palmgren. Die Lebensdauer von Kugellagern. *VDI Zeitschrift*, 68:339–341, 1924.

[12] X. Pitoiset and A. Premount. Spectral methods for multiaxial random fatigue analysis of metalic structures. *International Journal of Fatigue*, 22:541–550, 2000.

[13] I. Rychlik. A new definition of the rainflow cycle counting method. *Int. J. Fatigue*, 9:119–121, 1987.

[14] I. Rychlik. Note on cycle counts in irregular loads. *Fatigue and Fracture of Engineering Materials and Structures*, 16:377–390, 1993.

[15] I. Rychlik. Note on modeling of fatigue damage rates for non-gaussian stresses. Technical Report 2012:13, Mathematical Sciences, Chalmers, 2012.

[16] I. Rychlik, P. Johannesson, and M.R. Leadbetter. Modelling and statistical analysis of ocean-wave data using transformed gaussian processes. *Marine Structures*, 10:13–47, 1997.

[17] M. Shinozuka. Simulation of multivariate and multidimensional random processes. *J. Acoust. Soc. Am.*, 49:357–368, 1971.

[18] S.R. Winterstein. Non-normal responses and fatigue damage. *ASCE Journal of Engineering Mechanics*, 111:1291–1295, 1985.

[19] S.R. Winterstein. Nonlinear vibration models for extremes and fatigue. *ASCE Journal of Engineering Mechanics*, 114:1772–1790, 1988.

A Cross-moments of multivariate LMA's

In this section we use the notation for the loads introduced in (13), (25), and (26). We present some formulas for variance, kurtosis, and cross-correlations for $X_r(t)$, $X_{rk}(t) = \sum_{i=1}^{k} Z_{ir}(t)$, $r = 1, \ldots, M$. We start with an auxiliary formula that is straightforward to derive and valid for each positive u and v:

$$\mathsf{E}\left[(K_{ir}^*)^u (K_{is}^*)^v\right] = \nu_r^u \nu_s^v \Gamma(u+v+1) \left(\frac{T}{T+u\nu_r+v\nu_s}\right)^i, \tag{39}$$

$$\mathsf{E}\left[(K_{ir}^*)^u (K_{js}^*)^v\right] = \nu_r^u \nu_s^v \Gamma(u+1)\Gamma(v+1) \left(\frac{T}{T+u\nu_r+v\nu_s}\right)^i \left(\frac{T}{T+v\nu_s}\right)^{j-i}, \quad j > i. \tag{40}$$

Below, we only use (39), while (40) is provided for the completeness.

Recall that g_r, $r = 1, \ldots, M$, $T > 0$, and t are all chosen so that

$$\int_0^T g_r^2(t-u)\, du \approx \int_{-\infty}^{\infty} g_r^2(u)\, du = 1.$$

As a consequence of this, given that $v+t$ and v are within the range of t for which the above approximation is valid, is that $g_r * \tilde{g}_s(t) \approx \int_0^T g_r(v+t-u) g_s(v-u)\, du$, which is used in the calculations below. Therefore from now on we assume that T, t, v are chosen so that these approximations are valid.

We have

$$\begin{aligned} \frac{\mathbb{V}arX_{rk}(t)}{\mathbb{V}arX_r(t)} &= 1 - \int_0^T g_r^2(t-u)\, du \left(\frac{T}{T+\nu_r}\right)^k \\ &\approx 1 - e^{-\nu_r k/T}, \end{aligned} \tag{41}$$

where the approximation is accurate for large k.

We use (39) to compute the cross-correlation between X_r and X_s. Recall that $Z_{ir}(t) = \tilde{Z}_{ir}\sqrt{K_{ir}^*} g_r(t-U_i)$, with $\tilde{\mathbf{Z}}_i = (\tilde{Z}_{i1}, \ldots, \tilde{Z}_{iM}) = \sqrt{\mathbf{\Sigma}}\mathbf{Z}$, where $\mathbf{Z}$ is a standard normal vector. We obtain

$$\begin{aligned} \mathbb{C}ov(X_{rk}(v+t), X_{sk}(v)) &= \mathbb{C}ov(\tilde{Z}_{ir}, \tilde{Z}_{is}) \frac{1}{T} \int_0^T g_r(t-u) g_s(-u)\, du \sum_{i=1}^{k} \mathsf{E}\left[{K_{ir}^*}^{1/2} {K_{is}^*}^{1/2}\right] \\ &= \sigma_{rs}\sqrt{\nu_r\nu_s} \cdot \frac{1}{T} \int_0^T g_r(t-u) g_s(-u)\, du \sum_{i=1}^{k} \left(\frac{T}{T+(\nu_r+\nu_s)/2}\right)^i \\ &\approx 2\sigma_{rs} \frac{\sqrt{\nu_r\nu_s}}{\nu_r+\nu_s} \left(1 - \left(\frac{2T}{2T+\nu_s+\nu_r}\right)^k\right) g_r * \tilde{g}_s(t) \end{aligned} \tag{42}$$

and by passing with k to infinity

$$\mathbb{C}ov(X_r(t), X_s(0)) \approx 2\sigma_{rs} \frac{\sqrt{\nu_r\nu_s}}{\nu_r+\nu_s} g_r * \tilde{g}_s(t) \tag{43}$$

B Scaling property of expected damage for LMA loads

Here, we explain how the scaling property of the Laplace motion translates to the scaling property of the expected damage for the LMA model – the result that has been formulated in Proposition 1. Let

$\Lambda_\nu(t)$ be the Laplace motion given in (11) and consider $\tilde{\Lambda}(t) = \Lambda_\nu(\alpha t)/\sqrt{\alpha}$. We note that by using the series expansion (11) of $\Lambda_\nu(t)$, the process $\tilde{\Lambda}(t)$ can be rewritten with $\tilde{U}_i = U_i/\alpha$ which are distributed over $[0, \tilde{T}]$, where $\tilde{T} = T/\alpha$ yielding for $\tilde{\Lambda}$ the representation (11) with $\tilde{\nu} = \nu/\alpha$ or writing it in a compact manner

$$\Lambda_{\nu/\alpha}(t) = \Lambda_\nu(\alpha t)/\sqrt{\alpha},$$

where the equality is understood in the distributional sense.

Consequently, the LMA process $X_{s,\nu}(t)$ with a kernel $g_s(t) = g(t/s)/\sqrt{s}$ and driven by the Laplace motion (11) with the parameter ν satisfies

$$\begin{aligned} X_{\alpha s,\nu}(t) &= \int_{-\infty}^{\infty} g_{\alpha s}(t-u)\, d\Lambda_\nu(u) \\ &= \int_{-\infty}^{\infty} g\left(\frac{t}{\alpha s} - \frac{u}{\alpha s}\right) \frac{\sqrt{\alpha}}{\sqrt{\alpha s}}\, d\Lambda_{\nu/\alpha}\left(\frac{u}{\alpha}\right) \\ &= \int_{-\infty}^{\infty} g_s(t/\alpha - w)\, d\Lambda_{\nu/\alpha}(w) \\ &= X_{s,\nu/\alpha}(t/\alpha), \end{aligned}$$

where the second equality is again in the sense of probability distributions.

From this it follows that the rainflow cycles for $X_{s,\nu}$ computed over the interval $[0, T]$ are the same as those for $X_{\nu/s} = X_{1,\nu/s}$ computed over $[0, T\nu]$. Thus in view of (2) we have

$$D_\beta^{X_{s,\nu}}(a) = \frac{a^\beta}{s} D_\beta^{X_{\nu/s}}(1)$$

and by taking the expected value, this relation carries over to the expected damages as presented in (20).

C Expected damage for multivariate LMA loads

Let $Y(t)$ be a linear combination of some coordinates a multi-axial load as defined by (1), where $X_j(t)$, $j = 1, \ldots, M$ are given by (25). It follows directly from (25) that $Y(t)$ conditionally on the variance of transients K_{ij}^* and their locations $\mathbf{U} = (U_i)$ is a Gaussian (non-stationary) process. Since K_{ij}^*'s are random only due to $\mathbf{W} = (W_i)$ and $\mathbf{\Gamma} = (\gamma_i)$, we can write this conditional process as

$$Y^{\mathbf{w},\mathbf{u},\boldsymbol{\gamma}}(t) = \sum_{j=1}^{M} a_j X_j^{\mathbf{w},\mathbf{u},\boldsymbol{\gamma}}(t),$$

in which $X_j^{\mathbf{w},\mathbf{u},\boldsymbol{\gamma}}(t)$ are non-stationary Gaussian process depending on (now non-random) realizations of $\mathbf{W}, \mathbf{U}, \mathbf{\Gamma}$. Using this notation one can formally write the expected damage as

$$\mathcal{D}_\beta^{\mathbf{X}}(\mathbf{a}) = \mathsf{E}\left[\mathsf{E}\left[D_\beta^{\mathbf{X}}(\mathbf{a})|\mathbf{W}, \mathbf{U}, \mathbf{\Gamma}\right]\right] = \int D_\beta^{\mathbf{X}^{\mathbf{w},\mathbf{u},\boldsymbol{\gamma}}}(\mathbf{a})\, dP(\mathbf{w}, \mathbf{u}, \boldsymbol{\gamma}),$$

where $dP(\mathbf{w}, \mathbf{u}, \boldsymbol{\gamma})$ is the probability distribution of $(\mathbf{W}, \mathbf{U}, \mathbf{\Gamma})$. Despite this 'quasi'-explicit form of the expected damage, computing it would be a formidable task. For example if one attempts to use Gaussianity of $\mathbf{X}^{\mathbf{w},\mathbf{u},\boldsymbol{\gamma}}$ the main challenges are: these processes are non-stationary (although Gaussian), the conditional damages depend both on $\mathbf{a}$ and on $(\mathbf{w}, \mathbf{u}, \boldsymbol{\gamma})$, and they would have to be averaged according to the distribution of $(\mathbf{W}, \mathbf{U}, \mathbf{\Gamma})$. Essentially such an approach would amount to numerical evaluation through the Monte Carlo method.

However, if we assume that $\nu_r = \nu$, and $g_r(t) = g(t)$, $r = 1, \ldots, M$, then

$$\begin{aligned} Y(t) =& \sum_{i=1}^{\infty} \sqrt{\nu e^{-\nu\gamma_i/T} W_i} \cdot g(t - U_i) \sum_{r=1}^{M} a_r \tilde{Z}_{ir} \\ =& \sqrt{\mathbf{a}^T \mathbf{\Sigma} \mathbf{a}} \sum_{i=1}^{\infty} \sqrt{K_i^*} Z_i \cdot g(t - U_i), \end{aligned}$$

where the second equality is of distributions. Here Z_i's are independent standard normal variables. If we denote $X(t) = \sum_{i=1}^{\infty} \sqrt{K_i^*} Z_i \cdot g(t - U_i)$, we obtain the following simple relation between the expected damage of multi-axial load and uni-axial load

$$\mathcal{D}_\beta^{\mathbf{X}}(\mathbf{a}) = \mathcal{D}_\beta^X \left(\sqrt{\mathbf{a}^T \mathbf{\Sigma} \mathbf{a}} \right) = \left(\mathbf{a}^T \mathbf{\Sigma} \mathbf{a} \right)^{\beta/2} \mathcal{D}_\beta^X(1).$$

Therefore, for a given kernel g, computation of the expected damage for any $\mathbf{a}$, $\mathbf{\Sigma}$, and ν reduces to finding the expected damage of X as a function of ν, which is a significant simplification of the original problem.

D MATLAB code to simulate multi-axial correlated Hybrid model

For readers convenience we present the MATLAB codes used to simulate standardized (zero mean variance one) multi-axial hybrid model having exponential spectrum. We consider a three dimensional load. In the code some functions from the statistical toolbox in MATLAB are used. If the statistical toolbox is not available, then equivalent functions from the WAFO [7] toolbox at `www.maths.lth.se/matstat/wafo/` can be downloaded free of charge. Note that the WAFO toolbox contains also functions computing rainflow ranges that are used to estimate the fatigue damage index.

We will simulate tri-axial load saved in `X` on interval $[-T, T]$ with sample step `dt`. First the discretization step and related constants are set:

```
>> dt=0.001;  T=120; N0=floor(T/2/dt); N=2*N0+1;
>> t=0.5*linspace(-T,T,N)';
```

We now evaluate the kernel (`g`) and its transfer function (`Gk`), see (6). As in Example 1 we let $s = 0.034$.

```
>> w=pi/dt*linspace(-1,1,N)'; w3=[w w w]; K=3;
>> dw=w(2)-w(1); s=0.034;
>> S=0.5*s*exp(-s*abs(w3));
>> Gk=ifftshift(sqrt(S))/sqrt(dt/dw/N);
>> g=fftshift(real(ifft(Gk)));
```

The values of the parameter ν defining the Laplace noise are saved in the vector `nu`. Here we shall use $\nu = 0.002, 0.1, 0.077$ giving LMA's with kurtosis $3.14, 10, 8.4$, respectively.

```
>> nu = [0.002; 0.1;  0.077 ];
>> intg=trapz(t,g)';
```

In the following script one defines the covariance structure of the hybrid model. First the intensity of transients μ will be given, then the correlation matrices for jump sizes (`SIGMA`) and the correlation of added Gaussian noise (`CG`) will be specified.

```
>> SIGMA = [1 0 0; 0 1  0.7;  0  0.7 1 ]; CG=eye(3);
>> [V,D] = eig(SIGMA); AJump=V*sqrt(D);
>> [V,D] = eig(CG); AGauss=V*sqrt(D);
>> mu=500;
```

Now we turn to the the simulation algorithms of the multi-axial hybrid model. Basically the code is an implementation of (25-31), where the simulated load is given in the matrix `X`;

```
>>  X = zeros([N K]);
>>  Njmp=min(floor(mu*T),N);
>>  nu_min=min(nu);
>>  G = exp(-nu_min*cumsum(exprnd(1,1,Njmp))/T);
>>  W = sqrt(exprnd(1,1,Njmp));
```

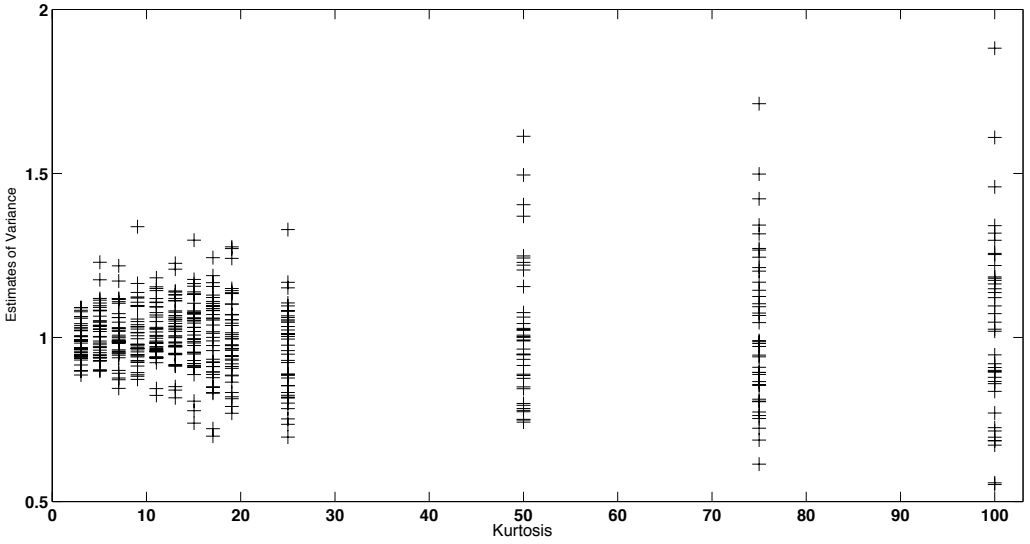

Figure 7: Variability of estimates of variances as a function of kurtosis for the hybrid model with the intensity $\mu = 500$ and the exponential kernel with $s = 1$. 1555 time units sampled with $dt = 0.2222$ were simulated, an equivalent of 14 seconds measurement of the cultivator force with $dt = 0.002$ and $s = 0.009$. On the x-axis we have kurtosis and on the y-axis the estimated variances of the simulated forces. (The observed kurtosis in cultivator signals was on average 11.5).

```
>>  Z = AJump*normrnd(0,1,[K Njmp]);
>>  dXG=sqrt(dt)*AGauss* normrnd(0,1,[K N]);
>>  indU=randperm(N);
>>  for ii=1:K
>>        nui=nu(ii);
>>        p=sqrt(exp(-nui*Njmp/T));
>>        dLambda=zeros(1,N);
>>        dLambda(1,1:Njmp) = sqrt(nui)*Z(ii,:).*W.*G.^(nui/nu_min/2);
>>        dLambda=dLambda(indU)';
>>        dX = p*dXG(ii,:)'+dLambda;
>>        X(:,ii) = real(ifft(Gk(:,ii).*fft(dX)));
>>  end
```

We finish with some practical remarks on applications of the presented program to simulate the multivariate hybrid model.

- It is assumed that the variance of the hybrid model is approximately one. The factors p, defined in (41), are introduced to compensate for the bias introduced by truncating the infinite series to k terms. However it should be noted that it does not remove variability of the estimates of the variance from the simulated samples of the hybrid process caused by finite time lengths of a simulated process. For short simulation periods T variability of the estimated variances is not negligible and increases with the value of ν (kurtosis). This is well illustrated in Figure 7 were simulated variances as function of kurtosis are presented. (Note that in general the growth rate also depends also on the shape of a kernel because of the relation (8) between ν and kurtosis.)

- In the simulations presented in Section 7 the intensity of transients was set to $\mu = 500$ [Hz], which basically means that the LMA and not hybrid models were used. Hence ν could be estimated using the relation (8). Now for lower intensity μ, i.e. when parameters p in (41) are non-zero, the relation (8) is no longer valid and can not be used to estimate ν. In the subsection below we show how the coefficients of kurtosis should be adjusted to estimate parameter ν in such a case.

- For high intensity μ of transients, it can happen that k is larger than the number of simulated times of the hybrid process. Extension of the program to cover such situations is straightforward, however for transparency of the code we do not present it here.

D.1 Kurtosis for the hybrid model

Recall that if $X(t)$ is a LMA process (9) with a kernel g, then the excess kurtosis of $X(t)$ is given from (8) by

$$\kappa_e(X(t)) = 3\nu \int g(t)^4 \, dt. \tag{44}$$

The series representation approximates $X(t)$ through

$$\nu \sum_{i=1}^{\infty} Z_i W_i e^{-\nu\Gamma_i/T} g(U_i - t) \tag{45}$$

and this approximation is utilized in the hybrid model (22) which we write here as

$$X_H(t) = X_k(t) + pZ_0(t),$$

where $Z_0(t)$ is the Gaussian part and

$$X_k(t) = \nu \sum_{i=1}^{k} Z_i W_i e^{-\nu\Gamma_i/T} g(U_i - t),$$

while p is chosen so that variances of the full series and the hybrid model agree.

In the paper we have focused on the case when the parameter ν is estimated from (9) since for the discussed data there was no need for adding the Gaussian component, i.e. $p \approx 0$ or, equivalently, the intensity μ of the transients per time unit is very large (recall that $p^2 = \exp(-\mu\nu) \approx (1 + \nu/T)^{-k}$, where $T = k/\mu$ is the observation time). In the full generality however, if the meaningful hybrid model is considered, we should work rather with the kurtosis of the hybrid model, which has to be worked out. Here we present its derivation.

Recall that if the distribution of (X, Y) is either the same as that of $(X, -Y)$ (or $(-X, Y)$) so that any $\mathsf{E}\left[X^m Y^{2k-1}\right]$ ($\mathsf{E}\left[X^{2k-1} Y^m\right]$), $k \in \mathbb{N}$ vanishes, then the following formula hold for the kurtosis of the sum of random variables

$$\kappa_e(X + Y) = \frac{6\rho + r\kappa_e(X) + r^{-1}\kappa_e(Y)}{2 + r + 1/r}, \tag{46}$$

where $r = \mathbb{V}ar(X)/\mathbb{V}ar(Y)$ and $\rho = \mathbb{C}ov(X^2, Y^2)/(\mathbb{V}ar(X)\mathbb{V}ar(Y))$. In particular, if X is Gaussian (so that $\kappa_e(X) = 0$) and independent of Y, then

$$\kappa_e(X + Y) = \frac{\kappa_e(Y)}{(r + 1)^2}.$$

Applying this to the hybrid model we obtain

$$\kappa_e(X_H(t)) = (1 - p^2)^2 \kappa_e(X_k(t)). \tag{47}$$

It remains to evaluate $\kappa(X_k(t))$. To this end let us denote $R(t) = X(t) - X_k(t)$ and note that by (46) we have

$$\kappa_e(X(t)) = \frac{6\rho + r\kappa_e(R(t)) + r^{-1}\kappa_e(X_k(t))}{2 + r + 1/r}, \tag{48}$$

where $r = p^2/(1 - p^2)$ and

$$\rho = \frac{\mathbb{C}ov(R^2(t), X_k^2(t))}{p^2(1 - p^2)}.$$

We first note that from the series representation (45):

$$R(t) = \nu e^{-\nu\Gamma_k/T} \sum_{j=1}^{\infty} \tilde{Z}_j \tilde{W}_j e^{-\nu\tilde{\Gamma}_j/T} g(\tilde{U}_j - t),$$

where $\tilde{Z}_j = Z_{k+j}$, $\tilde{W}_j = W_{k+j}$, $\tilde{U}_j = U_{k+j}$, $\tilde{\Gamma}_j = \Gamma_{k+j} - \Gamma_k$. Consequently,

$$\mathsf{E}\left[R^m(t)\right] = \mathsf{E}\left[e^{-m\nu\Gamma_k/T}\right] \cdot \mathsf{E}\left[X^m(t)\right] = \frac{T^k}{(m\nu + T)^k} \cdot \mathsf{E}\left[X^m(t)\right] \approx e^{-m\nu\mu} \mathsf{E}\left[X^m(t)\right]$$

and thus

$$\kappa_e(R(t)) \approx \kappa_e(X(t)).$$

Using this approximaton in (48), we obtain

$$\begin{aligned} \kappa_e(X_k(t)) &= (2r+1)\kappa_e(X(t)) - 6\rho r \\ &\approx \frac{3}{1-p^2}\left(\nu(1+p^2)\int g^4(t)\,dt - 2\rho p^2\right) \\ &= \frac{3}{1-e^{-\nu\mu}}\left(\nu\int g^4(t)\,dt + e^{-\nu\mu}(\nu - 2\rho)\right). \end{aligned} \tag{49}$$

Tedious but straightforward calculation yields

$$\begin{aligned} &\mathbb{C}ov(R^2(t), X_k^2(t)) \approx \\ &\approx \nu^4 \frac{\int g^2(t)\,dt}{T}\left(\frac{T}{2\nu+T}\right)^k \left(2\nu\left(1 - \left(\frac{2\nu+T}{4\nu+T}\right)^k\right) - T\left(\left(\frac{T}{2\nu+T}\right)^k - \left(\frac{2\nu+T}{4\nu+T}\right)^k\right)\right) \\ &\approx \frac{2\nu^3 e^{-2\nu\mu}}{T}\left(1 - e^{-2\nu\mu}\right) \end{aligned}$$

and thus

$$\rho \approx \frac{2\nu^3 e^{-\nu\mu}}{T}\left(1 + e^{-\nu\mu}\right).$$

Substituting this to (49) yields

$$\kappa_e(X_k(t)) \approx \frac{3\nu}{1-e^{-\nu\mu}}\left(\int g^4(t)\,dt + e^{-\nu\mu}\left(1 - \frac{4\nu^2}{T}e^{-\nu\mu}(1+e^{-\nu\mu})\right)\right).$$

Finally, substituting the above to (47) yields

$$\begin{aligned} \kappa_e(X_H(t)) &\approx 3\nu(1-e^{-\nu\mu})\left(\int g^4(t)\,dt + e^{-\nu\mu}\left(1 - \frac{4\nu^2}{T}e^{-\nu\mu}(1+e^{-\nu\mu})\right)\right) \\ &\approx 3\nu(1-e^{-\nu\mu})\left(\int g^4(t)\,dt + e^{-\nu\mu}\right), \end{aligned}$$

where the last approximation is valid because T is assumed to be large and is equivalent to considering $\rho \approx 0$. In practice, this equation should be used in order to get an estimate of ν (given μ) from the sample excess kurtosis. No explicit solution for ν is available but the solution can be easily obtained through standard numerical approximations.